REPORT DOCUMENTATION PAGE

Form Approved
OMB No. 0704-0188

PLEASE DO NOT RETURN YOUR FORM TO THE ABOVE ADDRESS.

1. REPORT DATE *(DD-MM-YYYY)*	2. REPORT TYPE	3. DATES COVERED *(From - To)*
08-26-04	Annual Report	Sep. 1, 2003-Aug. 31, 2004

4. TITLE AND SUBTITLE
Creep Behavior of Polymer Precursor Derived Si3N4/SiC Nanocomposites
Annual Report

5a. CONTRACT NUMBER

5b. GRANT NUMBER
N00014-03-1-0148

5c. PROGRAM ELEMENT NUMBER

6. AUTHOR(S)
Mukherjee, Amiya K.; Zhou, Xinzhang; and Hulbert, Dustin M.

5d. PROJECT NUMBER

5e. TASK NUMBER

5f. WORK UNIT NUMBER

7. PERFORMING ORGANIZATION NAME(S) AND ADDRESS(ES)
Department of Chemical Engineering and Materials Science
University of California
One Shields Avenue
Davis, CA 95616

8. PERFORMING ORGANIZATION REPORT NUMBER

9. SPONSORING/MONITORING AGENCY NAME(S) AND ADDRESS(ES)
Lawrence Kabacoff
Office of Naval Research
Ballston Centre Tower One
800 North Quincy Street
Arlington, VA 22217-5660

10. SPONSOR/MONITOR'S ACRONYM(S)
ONR

11. SPONSOR/MONITOR'S REPORT NUMBER(S)

12. DISTRIBUTION/AVAILABILITY STATEMENT
Approved for Public Release; distribution unlimited

20040917 127

13. SUPPLEMENTARY NOTES

14. ABSTRACT
Two batches of plasma sprayed zirconia-alumina-spinel powder (with or without high energy ball milling (HEBM)) were consolidated to full density by spark plasma sintering (SPS). The resulting nanocomposite showed superplasticity with a high activation energy of 945 kJ/mol for the HEBMed batch; the absence of HEBM treatment resulted in no superplastic behavior. The special grain boundary formed during SPS from nucleation and growth of new phases from metastable matrix in plasma sprayed powder is believed the key microstructure to turn this superplastic triphase ceramics into a non-superplastic one. If TEM analysis currently in process proves our postulation, plasma spraying may be a potential technique to make intrinsically creep-resistant microstructures.

15. SUBJECT TERMS
Nanoceramics, creep and superplasticity, deformation mechanisms

16. SECURITY CLASSIFICATION OF:			17. LIMITATION OF ABSTRACT	18. NUMBER OF PAGES	19a. NAME OF RESPONSIBLE PERSON
a. REPORT	b. ABSTRACT	c. THIS PAGE		13	Amiya K. Mukherjee
					19b. TELEPHONE NUMBER *(Include area code)* 530-752-1776

Office of Naval Research: **Annual Technical Report**

Term: 09/01/03 – 08/31/04

Contact Information

Contract Number	N00014-03-0148
Title of Research	Creep Behavior of Polymer Precursor Derived Si_3N_4/SiC Nanocomposites
Principle Investigator	Amiya K. Mukherjee
Organization	Department of Chemical Engineering and Materials Science, University of California, Davis

Technical Section

Technical Objectives

This project focuses on rate controlling mechanisms of nanoceramics at elevated temperatures. Earlier work supported by ONR related to investigation of creep mechanisms of SiCN nanoceramics by pyrolysis of a polymer precursor. Last year, we reported superplastic behavior at strain rates as high as 10^{-1} s^{-1} and at temperatures as low as 1300°C in zirconia-alumina-spinel triphase ceramic composites by spark plasma sintering of commercially available nanopowder mixtures. For comparison, Japanese work published in the journal *Nature* for the same composites needed a rather high temperature (1650°C) to realize a similar strain rate.

Plasma sprayed powders typically contain supersaturated solid solutions, higher temperature metastable phases and even amorphous contents. It has a strong driving force to reach equilibrium and might help the consolidation process.

After receiving from Professor B. H. Kear (Rutgers) the plasma sprayed triphase powder, we started consolidation of the compact spark plasma sintered from the powder with or without high energy ball milling (HEBM). No advantage of the plasma sprayed powder over nanopowder mixtures were shown in the SPS process. The superplastic behavior of the composites processed from plasma sprayed powders were compared with that processed from nanopowder mixtures. It was found that the new grain boundary formed during sintering by nucleation and growth of α alumina and spinel from the metastable supersaturated zirconia matrix. Thus, the grain boundary could be low angle and low energy and not intrinsically prone to slide. HEBM played a role in breaking up those special grain boundaries and improved grain boundary sliding.

Technical Approaches and Results

Superplasticity of zirconia-alumina-spinel nanoceramic composite by spark plasma sintering of plasma sprayed powders

Xinzhang Zhou[a], Dustin M. Hulbert[a], Joshua D. Kuntz[a], Rajendra K. Sadangi[b], Vijay Shukla[b], Bernard H. Kear[b] and Amiya K. Mukherjee[a*]

[a]Department of Chemical Engineering and Materials Science
University of California, Davis, CA 95616
[b]Center for Nanomaterials Research, Department of Ceramic and Materials Engineering
Rutgers University, Piscataway, NJ 08854

Abstract

Zirconia 3mol% yttria-alumina-alumina magnesia spinel nanoceramic composite was synthesized by spark plasma sintering of plasma sprayed particles. For compacts sintered from high energy ball milled powders, superplasticity was observed at temperatures between 1300 °C to 1450 °C and at strain rates between 10^{-4} s^{-1} and 10^{-2} s^{-1}, while for those without high energy ball milling, deformation at the same temperature and strain rate range did not show superplastic behavior. Also, the apparent activation energy (945 kJ/mol) of the high energy ball milled batch was much higher than that of the same composite processed from nanopowder mixtures (621 kJ/mol). The flow stresses were also higher at the same temperatures and strain rates. The difference may be related to the unique low angle grain boundaries in the grains that nucleated and grew from the metastable phase inside the plasma sprayed agglomerate at elevated temperatures. Such boundaries were not intrinsically easy to slide.

Keywords: nanoceramics, superplasticity, plasma spray, spark plasma sintering (SPS), low angle grain boundary, high energy ball milling (HEBM)

1. Introduction

Superplasticity was first widely studied in metals and alloys. The constitutive relationship for superplastic deformation usually takes the form of the Mukherjee-Bird-Dorn Equation [1]:

$$\dot{\varepsilon} = A\frac{D_0 Gb}{kT}\left(\frac{b}{d}\right)^p\left(\frac{\sigma}{G}\right)^n e^{-\frac{Q}{RT}} \quad (1)$$

in which G is the elastic shear modulus, b is the Burger's vector, k is Boltzmann's constant, T is the absolute temperature, d is the grain size, p is the grain-size dependence coefficient, n is the stress exponent, Q is the activation energy, D_0 is the diffusion coefficient and R is the gas constant. The inverse of n is termed the strain rate sensitivity m. Grain boundary sliding is generally the predominant mode of deformation during the superplastic flow. Plastic deformation by grain-boundary sliding is generally characterized by n=2 (or m=0.5) and an apparent activation energy that is typically either equal to that for lattice diffusion or for grain-boundary diffusion.

From Eq. (1), it is clear that at a constant temperature and stress, high strain rate is more easily realized in specimens with smaller grains. With the development of ceramic processing, the particle sizes are now made increasingly smaller into the nanometer range and so is the probability of realizing increasingly finer grain sizes in dense compacts. Superplasticity in ceramics has also been studied since the first observation of fine-structure superplasticity in yttria-stabilized tetragonal zirconia (YTZP) by Wakai in 1986 [2]. A number of fine-grained polycrystalline ceramics have also demonstrated superplasticity, such as YTZP [3], magnesia-doped alumina [4], and alumina reinforced YTZP [5]. Unfortunately, the superplastic temperatures were typically above 1450°C and the strain rates were relatively low (10^{-4} s^{-1} or lower). Recently, Kim, *et al* [6] realized a high strain rate of 0.1 s^{-1} in zirconia with 3mol% yttria-alumina-(alumina magnesia) spinel (ZAM) triphase composite (volume ratio 4:3:3), but at a rather high temperature of 1650°C.

More recently, superplasticity of the ZAM triphase ceramic composite at temperatures as low as 1300 °C was demonstrated in samples processed by spark plasma sintering (SPS) [7]. Because of rather low sintering temperature (1150 °C) and very short sintering time (3 minutes), the grain sizes of the three phases were between 50 *nm* and 100 *nm*. Superplastic behavior between 1300 °C and 1450 °C was observed with an apparent activation energy of 622 kJ/mol. Three binary systems of the triphase composite were also investigated to compare the sliding characteristic of three individual interfaces (zirconia-alumina, alumina-spinel and zirconia-spinel) [8]. It was concluded that in the triphase ceramic composite, zirconia-alumina and zirconia-spinel contributed more to the superplasticity (with the activation energies of 597 kJ/mol and 522 kJ/mol respectively). Although alumina-spinel was not superplastic, spinel played a roll in hindering the grain growth of the other two phases.

The above ceramic composites were processed by mechanically mixing nanoparticles and subsequent sintering. A new parallel process to make monolithic nanoceramic composites [9] is plasma spraying of spray dried aggregates of a mixture of different ceramic particles, followed by sintering of the plasma sprayed powders. The advantage of this method is that the nanophases in plasma sprayed powders are more uniformly distributed. This is due to high nucleation rates and limited grain growth of each phase from the liquid state in the unique plasma melting and fast quenching process [10]. Another advantage is that starting materials are not necessarily nanoparticles. A typical

spray dried particle composed of an aggregate of micrometer sized primary particles consisting of all components in the composite. In most cases, the plasma sprayed particles have large strain energies and usually contain metastable and even amorphous phases [10], which have a considerable driving force to form an equilibrium state and thus can help in consolidation. Duan et al studied the phase transformations in the consolidation by SPS of plasma sprayed metastable Al_2TiO_5 powder and of mixtures nano-Al_2O_3, TiO_2 powder with and without MgO additive [11]. This paper will discuss the consolidation of zirconia-alumina-spinel nanoceramic composite processed from plasma sprayed powders and high temperature deformation. Comparison will be made to the nanoceramic composite of the same composition processed from mechanically mixed commercially available nano particles.

2. Experimental Procedures

2.1 Spray Drying and Plasma Spraying

High purity starting powders for spray drying are TZ3Y (Tosoh, Japan), alumina (Baikowski Malokoff Inc., Malokoff, TX) and alumina magnesia spinel (Baikowski International Corp., Charlotte, NC). The average particle sizes are in either submicron meter or nanometer range. The powders were mixed in water (50 vol% solid loading) and ball milled for 24 hours. A Niro 2M spray drier (Niro Inc., Columbia, MD) was used to spray dry the slurry. The resulting agglomerate was sieved and only sizes between 35 and 75 micrometers were used as input of plasma spray. Plasma spraying was carried out using a Sulzer-Metco 9MP gun. The carrier gas was argon and the primary and secondary gases were respectively hydrogen and nitrogen. The current and voltage were 750 A and 65 V respectively. Plasma melted particles were quenched in a water bath. The process is discussed in detail elsewhere [10].

2.2 High Energy Ball Milling (HEBM)

Two batches of plasma sprayed powders were made for subsequent sintering. One (PS-HEBM-SPS) was first high energy ball milled for 24 hours in a SPEX 8000 mixer mill (SPEX CertiPrep, Metuchen, NJ) with a tungsten carbide (WC) ball in a WC vial. One wt% polyvinyl alcohol (PVA) was added as a dry milling agent to prevent severe agglomeration. A heat treatment in air at 350 °C for 3 hours after HEBM removed the PVA from the powder mixture. After sieving to remove the particles over 100 μm, the powders were unidirectionally pressed at 35 MPa in a graphite die (~20 mm in diameter) to form the green compacts. The other batch was directly consolidated without HEBM.

2.3 SPS

SPS is a new sintering method with moderate pressures and comparatively low temperatures [12]. Spark plasma is generated between the particles by electrical discharge at the onset of on-off DC pulsing. The on-off DC pulses may also result in spark impact pressure, Joule heating and electrical field diffusion. SPS can rapidly consolidate the green

compact to nearly theoretical density. In SPS, rapid heating rate (normally a few hundreds °C/min), moderate pressure and short sintering time (minutes) makes it possible to consolidate fully dense ceramics while retarding grain growth.

In this study, a Dr. Sinter 1050 (Sumitomo Coal Mining Co., Japan) was used to sinter the green compacts to full density. The heating rate was 300°C/min from room temperature to 600°C and then in 2 minutes the samples were ramped to 1150 °C. After holding at 1150 °C for 3 minutes, the power was shut down and the samples were cooled in vacuum. A unidirectional pressure of 63 MPa was applied during sintering and an optical pyrometer focusing on the graphite die monitored the temperatures. The final densities of sintered compacts were measured by the Archimedes method with deionized water as the immersion liquid. The theoretical densities were calculated by the rule of mixtures.

2.4 Mechanical Testing and Characterization

The sintered samples were cut and polished to a bar shape approximately 3 mm by 3 mm by 5 mm (height). Mechanical tests were carried out on a PC Labview controlled MTS-810 loading frame. Once the samples were heated up in air to the desired testing temperatures, strain rate-jump tests were conducted at a certain constant temperature. The specimen was deformed at a constant strain rate until a 0.1 true strain was reached before going on to the next strain rate. In our tests, a true strain of 0.1 in each step was enough to obtain a steady flow stress.

Phases were identified using a XDS 2000 X-ray diffraction (XRD) Diffractometer using Cu K_α radiation (Scintag Inc., Cupertino, CA). A FEI XL30-SFEG high resolution scanning electron microscope (SEM) (Philips, Germany) was used to observe the microstructures.

3. Results and discussion

3.1 Powder processing

For plasma sprayed powders, the phases were identified as metastable tetragonal zirconia, with Al and Mg atoms in a highly supersaturated solid solution (Fig. 1). When heat treated above 1200 °C, the metastable phase decomposed into a triphase composite.

A typical microstructure of the plasma sprayed particles is shown in Fig. 2a (low magnification) and Fig. 2b (high magnification). Spherical particles have a typical diameter from 1 to 20 micron meters, and at higher magnification, Fig. 1b shows the cellular segregated structure on the particle surface. The bright regions are Zr^{4+}-rich areas, while dark ones are Mg^{2+} and Al^{3+}-rich area. While tetragonal zirconia formed directly from the cellular core, nucleation of α alumina and spinel grains occurred in the segregated interstitices of the cellular structure. [13]

Powders treated with HEBM did not show difference in XRD or in fine microstructures; however, no spherical particles over a micrometer existed. This indicates that during HEBM, big plasma sprayed particles fractured into the sub micrometer range.

After unidirectional press in a graphite die, the relative green densities were around 45%-50% for both HEBM and non HEBM compacts.

3.2 SPS

The SPS parameters were optimized and were the same as those processed from mixtures of commercial nanopowders in Ref. [7]. All sintered compacts (termed PS-HEBM-SPS and PS-SPS for compacts from HEBM plasma sprayed powders and non HEBM ones) had a theoretical density over 99%. It seems that the nanostructured microstructures formed by rapid quenching and the high strain energy by HEBM did not further enhance the sinterability in SPS process. Lower temperatures (as low as 1100°C) or shorter sintering time (as short as 1 minute) resulted only 70%-85% theoretical density. The sintering kinetics may be related with the microstructures of plasma sprayed and quenched metastable particles. On one hand, the metastable phase has a large driving force to equilibrium. Because α alumina and spinel have lower densities than zirconia, nucleation and growth of α alumina and spinel from tetragonal zirconia instantly increased the compact density and thus enhanced consolidation. On the other hand, the grain boundaries formed inside the particles by nucleation and growth from the metastable phase may have preferred orientation, low angle and low energy and may have strong bonding between neighboring nanograins. As indicated by other authors on SPS of ceramics, most plasma discharges occurs between particles [12]. In this way, the strong bound grain boundaries formed inside the hard agglomerates did not contribute much to the sintering process. The fresh surfaces on the particles formed in HEBM were probably more active during SPS consolidation. The plasma spark between these fresh surfaces possibly activated stronger Joule heating and electrical field assisted diffusion, which enhanced the densification between the fresh surfaces. With the two contrary factors discussed above, the consolidation process of plasma sprayed powders showed little difference from that of the nanopowder mixtures.

3.3 Mechanical properties and microstructural analysis

A typical flow stress-strain graph of the jump test is shown in Fig. 3a for PS-HEBM-SPS specimen tested at 1450 °C. The flow stresses at different temperatures and strain rates are listed in Table I for ceramic composites from PS-HEBM-SPS, PS-SPS and the nanopowder mixture. It is obvious that the flow stresses of the sample with HEBM are much smaller than those without HEBM. In addition, all samples of PS-HEBM-SPS did not fracture up to a 0.51 total true strain while some of those PS-SPS specimens failed during the test. For comparison, the flow stresses process from nanopowder mixtures were also listed in Table I. The flow stresses are smaller than those processed from plasma sprayed powders with/without HEBM.

According to Eq. (1), the slope of a log (σ) vs. log ($\dot{\varepsilon}$) curve can give the strain rate sensitivity m, i.e. the inverse of the stress dependence of the strain rate, n. Fig. 3b shows the superplastic behavior for zirconia-alumina-spinel composite. The slope of each line is

around m=0.5, i.e. the stress exponent of the strain rate is equal 2. This clearly demonstrates superplasticity in the temperature and strain rate range tested. Therefore the grain or interface boundaries experienced substantial sliding during superplastic deformation.

From Eq. (1), the apparent activation energy Q can be derived at constant stresses from the slope of the Ln ($\dot{\varepsilon}$) vs. $1/T$. At constant stress the apparent activation energy of PS-HEBM-SPS is calculated from Fig. 3c. The average activation energy is 945 kJ/mol, which is much higher than that of the composite processed from nanopowder mixtures (622 kJ/mol) [7].

SEM images of the fracture surfaces of the deformed specimen (PS-HEBM-SPS) (Fig. 4A, C, E) show three kinds of different microstructures: equiaxed grains with round corners (Fig. 4A), deformed dense agglomerates (Fig. 4C), and non-deformed dense plasma sprayed agglomerates (Fig. 4E). The first kind of microstructure (Fig. 4A) is evidence of grain boundary sliding (perhaps with some grain boundary migration) and relates to superplasticity, which was typical of the microstructures in the deformed specimens processing from the nanopowder mixture. This type of structure is formed from the fine particles created in HEBM. The second type (Fig. 4C) is most likely from the medium size particles formed in HEBM. Because of short sintering time, the microstructures inside the hard particles were spared from large amounts of grain growth. Sintering most likely happened only between hard agglomerates and since the bonding between grains inside the agglomerate is strong, the whole agglomerate slid as one entity during deformation or deformed as one unit and changed its shape under stress. The third microstructure (Fig. 4E) is uncommon and it probably came from plasma sprayed particles not affected by HEBM and thus these particles kept their shape during SPS and deformation. Again the strongly bound grains inside hard agglomerates did not contribute to grain boundary sliding. Fig. 4B, D, F are for the deformed PS-SPS samples. It is just the extreme case of the third microstructures (Fig. 4E) with a larger amount of bigger hard agglomerates. The absence of HEBM in the processing route resulted in more and bigger hard agglomerates with strong bonding between the nanograins inside these agglomerates.

The difference in the superplastic behavior, especially in activation energy, implies different energetics of grain boundary sliding. The grains in the specimen processed from nanopowder mixtures are more random in orientation and the grain boundaries are more prone to have high angles and high energy. As a result, grain boundary sliding should be easier [13]. For plasma sprayed powders, the strong low grain boundaries between primary grains inside the particle formed by nucleation and growth from the metastable phase at elevated temperatures did not change during deformation. This suggests that the whole hard agglomerate acts as one entity during SPS and high temperature deformation. Therefore, the sliding unit is not individual grains, but the whole particle or hard agglomerate. This could explain the lack of superplasticity in PS-SPS specimens, i.e. the microstructure behaved as a course grained sample. The PS-HEBM-SPS specimens were superplastic because of smaller effective grain sizes but with a much higher apparent

activation energy than that of the specimens SPSed from nanopowder mixtures. Small impurity (e.g. W, Co from HEBM) segregation may significantly increase the apparent activation energy for the grain boundary diffusion. This could also be responsible for the observed high apparent activation energy in HEBMed samples. TEM studies on the grain boundaries of the deformed specimens are currently in progress to further substantiate the above analysis.

4. Conclusions

Nanoceramic composites were synthesized from HEBMed plasma sprayed nanoceramic zirconia-alumina-spinel powders by SPS. The samples were fully dense and showed superplasticity with an apparent activation energy of 940 kJ/mol at temperatures between 1300 °C and 1450 °C and strain rates between 10^{-4} s^{-1} and 10^{-2} s^{-1}. The grain boundaries formed inside plasma sprayed particles may have different properties other than those processed by nanopowder mixtures. The neighboring grains inside plasma sprayed agglomerates may have preferred orientation with low angle and low energy after nucleation and growth from metastable tetragonal zirconia at elevated temperatures. The actual sliding unit may be groups of grains formed inside plasma sprayed agglomerates, rather than the individual grains. This situation is then comparable to the deformation of a course grained matrix, which is not expected to demonstrate much superplastic ductility.

References

[1] A. K. Mukherjee, J. E. Bird, J. E. Dorn, ASM Trans. 62 (1969), 155-179.
[2] F. Wakai, S. Sakaguchi, Y. Matsuno, Adv. Ceram. Mater. 1 (1986), 259-263.
[3] T. G. Nieh, J. Wadsworth, Acta Metall. Mater. 38 (1990), 1121-1133.
[4] Y. Yoshizawa, T. Sakuma, Acta Metall. Mater. 40 (1992), 2943-2959.
[5] F. Wakai, H. Kato, Adv. Ceram. Mater. 3 (1988), 71-76.
[6] B. N. Kim, K. Hiraga, K. Morita and Y. Sakka, 413 (2000), 288-291.
[7] J. D. Kuntz, J. Wan, A. K. Mukherjee, to be submitted to Mat. Sci. Eng. A, 2004.
[8] X. Zhou, D. M. Hulbert, J. D. Kuntz, J. E. Garay and A. K. Mukherjee, in: Advances in Ceramic Matrix Composites X, ed. Singh, J. P., Ceram. Trans., 165, in press, (2004).
[9] B H. Kear, Z. Kalman, R. K. Sadangi, G. Skandan, J. Colaizzi, W. E. Mayo, J. Therm. Spray Technol. 9 (2000), 483-487.
[10] X. Zhou, V. Shukla, W. R. Cannon, B. H. Kear, J. Am. Ceram. Soc. 86(2003), 1415-1420.
[11] R. G. Duan, G. D. Zhan, J. D. Kuntz, B. H. Kear, A. K. Mukherjee, Mater. Sci. & Eng. A 373 (2004), 180-186.
[12] G. D. Zhan, J. D. Kuntz, J. Wan, A. K. Mukherjee, Nat. Mater. 2 (2003), 38-42.
[13] H. Kokawa, T. Watanabe, S. Karashima, Phil. Mag. A 44 (1981), 1239-1254.
[14] B. H. Kear, Xinzhang Zhou, R. K. Sadangi, S. Balasubramaniun, B. Mcenerney,

Monthly report for Nano-ceramic composites for heavy armor on MAGTF expeditionary family of fighting vehicles, August, 2002.

Table I flow stresses of the three ceramic composites
(A: nanopowder mixtures, B: PS-HEBM-SPS, C: PS-SPS)

Strain rate (s^{-1})	Flow stress (MPa)									
	1300 °C		1350 °C		1400 °C			1450 °C		
	A	B	A	B	A	B	C	A	B	C
$1x10^{-4}$	*	*	*	46	*	7	118	*	3	*
$3.16x10^{-4}$	*	74	*	22	*	11	170	*	5	*
$1x10^{-3}$	65	125	28	37	13	18	236	7	9	90
$3.16x10^{-3}$	127	216	56	61	24	30	!	13	16	149
$1x10^{-2}$	227	#	108	110	48	52	!	24	32	197

Notes: * not tested
beyond equipment load limit
! sample fractured during deformation

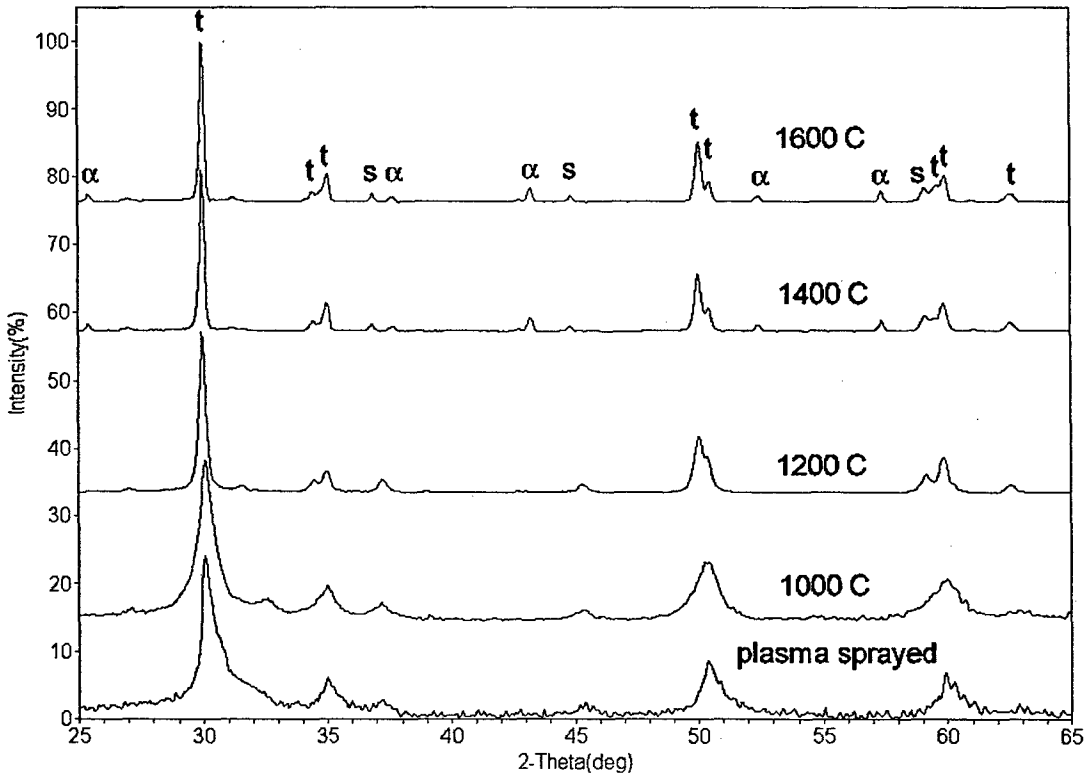

Fig. 1 XRD pattern of plasma sprayed powders and heat treatment effects
(t: tetragonal zirconia, α: α alumina, s: spinel)

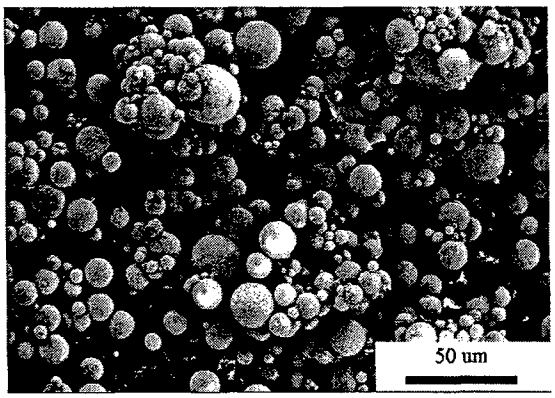

Fig.2a Plasma sprayed ZAM powders (low magnification)

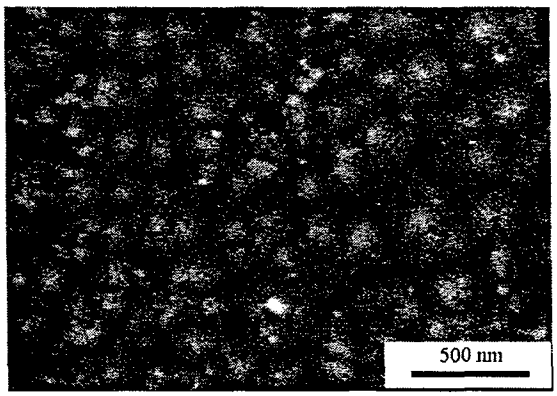

Fig. 2b Surface of a plasma sprayed ZAM powder (high magnification, showing details on a particle surface in Fig 1a)

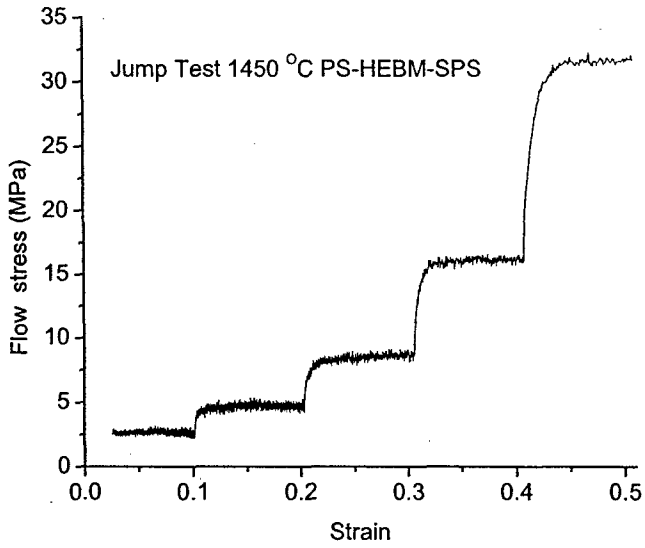

Fig. 3a Jump test of PS-HEBM-SPS specimen at 1450 °C

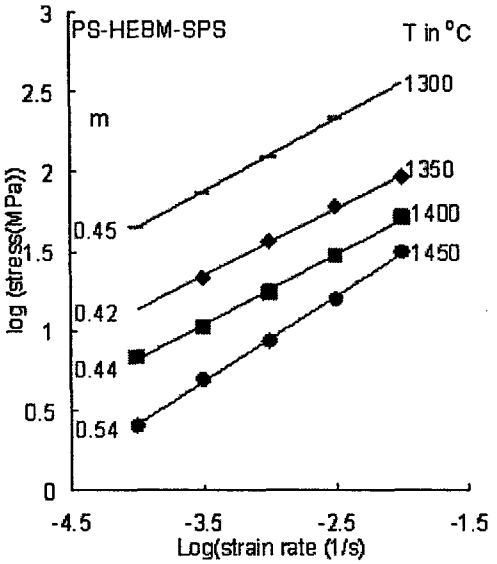

Fig. 3b Stress-strain curves in log-log scale to determine strain rate sensitivity m

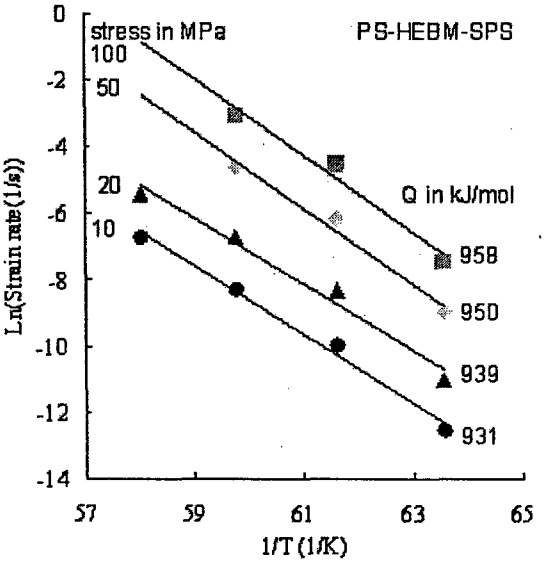

Fig. 3c log(strain rate)-1/T curves to determine the apparent activation energy Q

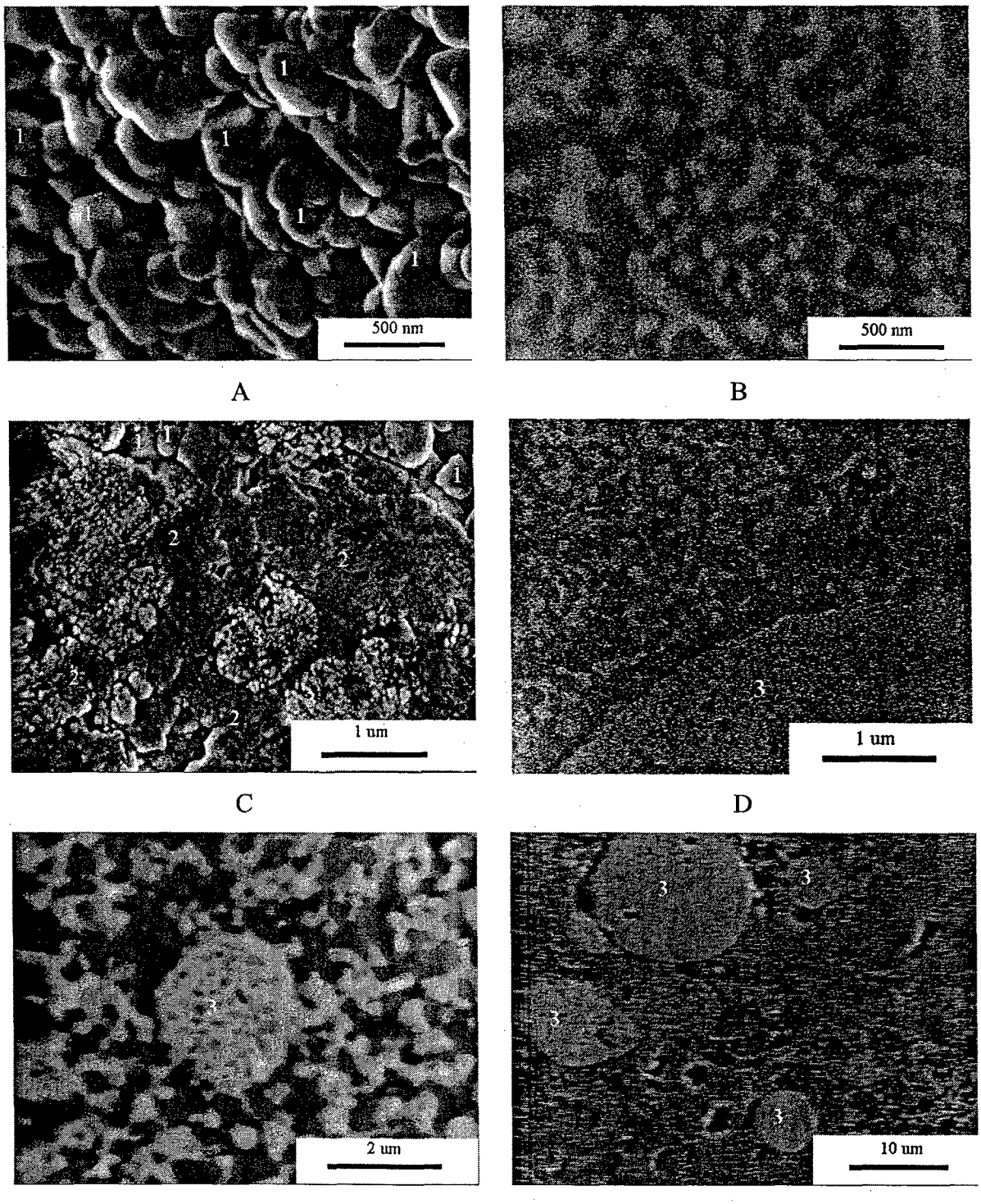

Fig. 4 SEM images of deformed PS-HEBM-SPS (A, C, E) and PS-SPS (B, D, F) at 1400 °C (Mark 1: grains with round corners; Mark 2: deformed hard agglomerates; Mark 3: not deformed hard agglomerate in spherical shape)